



## Research paper

# Gas network development in a precompacted bentonite experiment: Evidence of generation and evolution



Jon F. Harrington<sup>a,\*</sup>, Caroline C. Graham<sup>a</sup>, Robert J. Cuss<sup>a</sup>, Simon Norris<sup>b</sup>

<sup>a</sup> British Geological Survey, United Kingdom

<sup>b</sup> Radioactive Waste Management Ltd., United Kingdom

## ARTICLE INFO

## Keywords:

Bentonite  
Advection  
Multi-phase flow  
Deformation  
Permeability  
Radioactive waste

## ABSTRACT

In a deep geological disposal facility for radioactive waste, precompacted bentonite is proposed as a sealing material for the isolation of boreholes, disposal galleries and deposition holes. The advective movement of repository gas in bentonite has been linked to the development of new porosity and propagation of dilatant pathways. For the first time we present a detailed analysis of stress field data during the generation and evolution of a gas network. A new experimental dataset, from a highly instrumented test, clearly shows the strong coupling between stress, gas pressure and flow in bentonite. Multiple discrete propagation events are observed, demonstrating spatial variability and time-dependency as permeability within the clay develops. Analysis of the stress data before, during and after gas entry indicates a heterogeneous stress field initially develops, resulting from the development of these pathways. The flow network is dynamic and continues to spatially evolve after gas entry, such that permeability under these conditions must be time-dependent in nature. Perturbation of the stress field is significant before all major gas outflow events, presumably resulting from the requirement to propagate an effective gas network before outflow is possible. In contrast, no major flow perturbations are detected which did not correlate with fluctuations in the stress field. The controls on the distribution and geometry of the resulting flow network are unclear, as well as its long-term evolution and stability. These will be beneficial in the assessment of gas pressure evolution as part of safety case development.

## 1. Introduction

The deep geological disposal of radioactive waste presents a number of significant engineering challenges, not least understanding the fate and impact of waste-package derived gas on the engineered barrier systems (EBS) and host rock, which form an integral part of a geological disposal facility (GDF). Corrosion of ferrous materials under anoxic conditions, combined with the radioactive decay of waste and radiolysis of water, lead to the formation of hydrogen, carbon dioxide, hydrogen sulphide and methane within a repository depending on the waste composition, availability of water and disposal concept. Determination of the primary mode of gas migration is a complex issue, dependent on both repository concept and evolution. As such, there remains a degree of uncertainty as to the relative importance of diffusion versus advection. However, in scenarios where the rate of gas production exceeds the rate of gas diffusion through the EBS or host rock, a discrete gas phase will form (Weetjens and Sillen, 2006; Ortiz et al., 2002; Wikramaratna et al., 1993; Sellin and Leupin, 2013; SKB, 2006; Norris, 2015). Under these conditions, a free gas phase begins to accumulate

until its pressure becomes sufficiently large for it to move, through advection, in the surrounding material (Sellin and Leupin, 2013; Graham et al., 2012; Harrington and Horseman, 1999, 2003; Horseman et al., 1999). Previous studies (Angeli et al., 2009; Skurtveit et al., 2012; Harrington et al., 2009, 2012a,b; Cuss et al., 2014a,b; Gerard et al., 2014; Rodwell, 2000) indicate that in the case of plastic clays (Whitlow, 2001) and in particular precompacted bentonite, advective gas flow is associated with the development of new pressure induced pathways leading to a complex coupling between gas pressure, stress state and volumetric strain (Gensterblum et al., 2015; Amann-Hildenbrand et al., 2015; Cuss et al., 2014a,b; Harrington et al., 2012a, 2012b; Graham et al., 2012; Horseman and Harrington, 1994; Horseman et al., 1999; Harrington and Horseman, 2003; Romero et al., 2012; Marschall et al., 2005; Wiseall et al., 2015).

The phenomenon of dilatant flow is not new to geoscience. In early 1971, two French researchers Tissot and Pellet (1971) examining the mechanisms controlling primary hydrocarbon migration stated “The displacement of an oil or gas phase from the centre of a finely grained argillaceous matrix goes against the laws of capillarity and is in

\* Corresponding author.

E-mail address: [jfha@bgs.ac.uk](mailto:jfha@bgs.ac.uk) (J.F. Harrington).

principle impossible. The barrier can, however, be broken in one way. The pressure within the fluids formed in the pores of the source-rock increases constantly as products of the evolution of kerogen are formed. If this pressure comes to exceed the mechanical resistance of the rock, microfractures will be produced which are many orders of size greater than the natural (pore) channel of the rock, and will permit the escape of an oil or gas phase, until the pressure has fallen below the threshold which allows the fissures to be filled and a new cycle commences.” This hypothesis was supported by Mandl and Harkness (1987) who, independently of Tissot and Pellet (1971), suggested hydrocarbon migration only occurs through thick, continuous water-wet rocks of low permeability through a process of fracturing, forming what they call ‘dykelets’. Studies on subsea hydrocarbon seepages by Clayton and Hay (1992) and Judd and Sim (1998) suggest capillary displacement pressures are often so large, that the gas pressure required to initiate flow can approach or even exceed the local stress. These observations were supported by Donohew et al. (2000) who, examining gas migration processes in unconfined clay pastes of varying moisture content and mineralogy, observed the creation of dilatant, preferential pathways, the morphology of which was related to the plasticity and density of the clay.

Despite the evidence for pathway dilation and sealing, the exact mechanisms controlling gas entry and flow in clay-rich media remain poorly understood and the memory<sup>1</sup> of such pathways and their potential impact on barrier performance is uncertain.

This paper describes a highly instrumented and detailed test examining the interaction between gas pressure and stress during initial pathway generation and the development of permeability in an EBS consisting of saturated, precompacted bentonite. A detailed analysis of the stress field during gas network development is presented and the implications for radioactive waste disposal discussed.

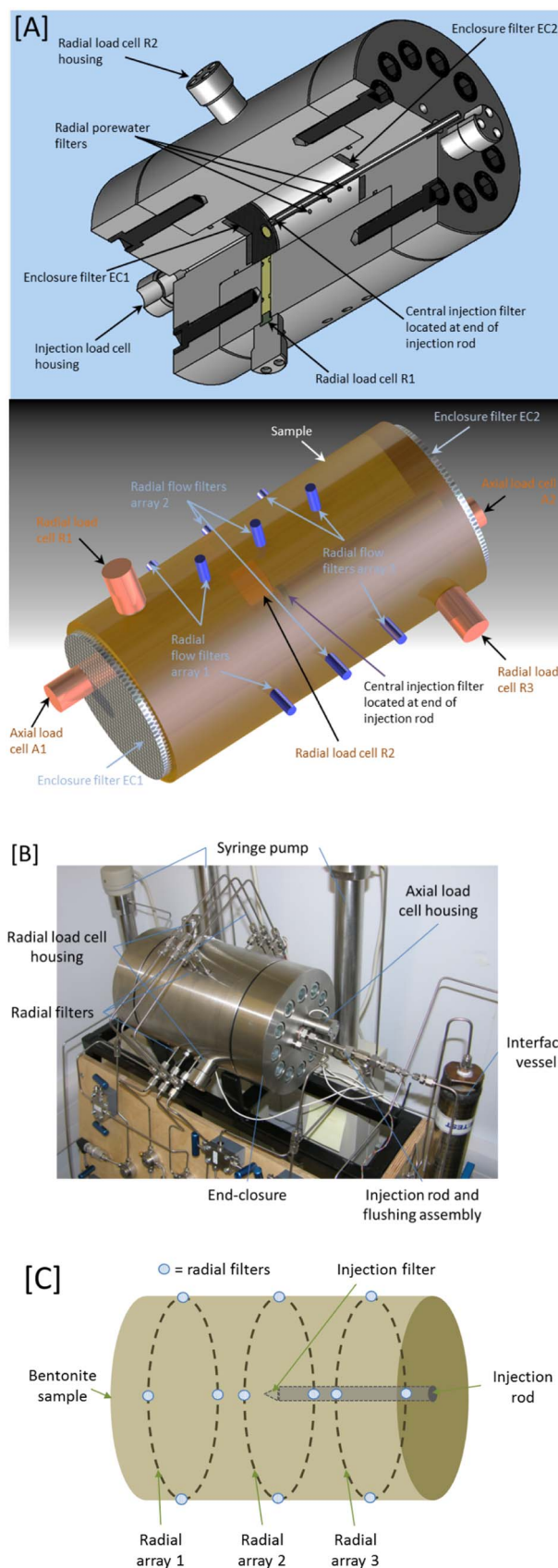
## 2. Apparatus

Conceptually, the apparatus reproduces some of the main features of the repository near-field within a hard host rock, including the deposition hole, a corroding canister generating gas and a number of conductive fractures in the host rock. Tests are performed in a constant volume apparatus which is a direct analogue for a radioactive waste repository within a hard (e.g. crystalline) host rock. The unyielding walls of the host rock confine the EBS which is used to encapsulate high-level radioactive waste containers (Sellin and Leupin, 2013). This boundary condition was selected for this test programme as it represents the favoured disposal concept in both Finland and Sweden, the two countries most advance in Europe in their development of an operational GDF.

In the configuration used in this study, there are five main components: (1) a thick-walled dual-closure stainless steel pressure vessel (representing the walls of the deposition hole), (2) a fluid injection system (simulating the generation of gas within the bentonite), (3) three independent backpressure systems (simulating conductive features intersecting the deposition hole), (4) five stress sensors to measure radial and axial stress and (5) a LabView™ based data acquisition system. Fig. 1A is a cut-away section showing both end-closures with their embedded drainage filters, EC1 and EC2 and axial stress sensors A1 and A2, the central fluid injection filter, the twelve radial sink filters, the three radial stress sensors (R1, R2 and R3) and the porewater pressure sensor. The central or “source” filter is mounted at the end of a 6.4 mm diameter stainless steel tube and is used to inject the permeant at the mid-point of the sample, either helium<sup>2</sup> or distilled water

<sup>1</sup> The term memory is used to describe a propensity for the re-establishment of a pathway at the same location despite prior closure.

<sup>2</sup> While hydrogen will be the primary gas generated in a GDF for high level waste and/or spent fuel, helium was selected as a safe substitute based on its inert nature and similar molecular diameter.



(caption on next page)

**Fig. 1.** [A] Cut-away schematic of the constant volume and radial flow (CVRF) gas migration apparatus used in this study from two perspectives showing the instrumentation. Note filters/load cells on the back of the vessel are not visible in these drawings. [B] Photograph of apparatus and tubing connections. [C] Schematic showing the location of the central gas injection filter and radial drainage arrays. The pressure and flow to each radial array (comprised of four separate filters) was controlled by a separate syringe pump. Sample dimensions are nominally 120 mm in length and 60 mm in diameter.

depending on the test stage. The end of the filter is profiled to match a standard twist drill. A 1.6 mm diameter tube passes down the bore of the filter tube to enable flushing of the tube prior to gas injection. Pressure and flow rate of test fluids are controlled or monitored using a pair of ISCO-260, Series D, syringe pumps operated from a single digital control unit. To avoid potential leakage of gas through pump seals, helium is displaced from an interface vessel during gas injection, Fig. 1B, by pumping deionised water from the injection pump. As such it should be noted that inflow to the system includes compression of the gas in the interface vessel.

Local stress was measured at five separate locations using load cells mounted on the outside of the vessel. Tungsten carbide rods (chosen for their high modulus) run through the wall of the vessel transmitting the force developed by the clay directly to the externally mounted load cells. As such, these units record the development of local stress in the clay i.e. the sum of swelling and porewater pressures. All load cell and pressure transducers are calibrated against a known laboratory standard. A programme written in LabView™ elicits data from the pump at pre-set time intervals, generally 120 s. Testing is performed in an air-conditioned laboratory at a nominal temperature of  $20 \pm 0.5$  °C.

### 3. Samples and procedures

Precompacted blocks of Volclay Mx80 bentonite (supplied by AMCOL International Corporation, USA) with a nominal dry density of  $1.56 \text{ Mg/m}^3$  were supplied by Clay Technology AB of Lund, Sweden. While a detailed analysis of its chemical composition can be found in Johannesson (2014), on average the material comprised (by percentage weight) 90.2% montmorillonite, 0.5% gypsum, 4.8% quartz, 0.1% calcite, 3.5% plagioclase and 0.9% muscovite. Upon receipt of the preserved bentonite blocks at BGS (sealed to prevent moisture loss and chemical reaction), the material was catalogued and stored under refrigerated conditions of 4 °C to minimise potential biological and chemical degradation. Off-cuts collected during sample preparation were weighed and oven dried to obtain an estimate of moisture content and initial geotechnical properties, Table 1.

A cylindrical test specimen, with diameter 60 mm and length 120 mm, was manufactured by machine lathing, with the end surfaces cut flat and parallel. A 6.4 mm diameter hole was then drilled in the clay, from one flat end surface, to the mid-point of the sample in order to accommodate the injection filter and tube. The specimen was then carefully inserted into the pressure vessel by hand, forming a snug fit with the internal bore of the vessel. Each end closure was located into place and the cap-head screws gently tightened to ensure contact between the sample and the end-closure. No significant axial pre-stress was applied to the samples. Once tube connections from the pumps to the end-closures had been made, the system was flushed with distilled water or helium gas (depending on the position of the filter) and the test was ready to begin.

**Table 1**

Basic physical properties of sample Mx80-A prior to testing. An assumed specific gravity for the mineral phases of  $2.77 \text{ Mg/m}^3$  was used in these calculations. Geotechnical properties are based on oven drying of material to 105 °C.

Sample	Moisture content (%)	Dry density ( $\text{Mg/m}^3$ )	Porosity	Void ratio	Saturation
Mx80-A	0.266	1560	0.437	0.776	0.95

**Table 2**

Summary of experimental history showing test stage, type of test, injection pressure and backpressure values and the start time in days of each test stage. Pressure ramp phases denote periods of testing where the injection pump is set to constant flow rate mode.

Test stage	Type	Injection pressure (MPa)	Backpressure (MPa)	Time (d)
1	Hydration	0.25	0.25	0
2	Hydration	1.0	1.0	8.3
3	Gas test	Pressure ramp	1.0	49
4	Gas test	3.0	1.0	75.6
5	Gas test	Pressure ramp	1.0	141.4
6	Gas test	6.5	1.0	162.9
7	Gas test	Pressure ramp	1.0	203.2
8	Gas test	7.25	1.0	209.2
9	Gas test	Pressure ramp	1.0	568.9
10	Gas test	7.73	1.0	581.3
11	Gas test	Pressure ramp	1.0	720.3

The test, designated Mx80-A, comprised a series of component stages (Table 2) designed to understand the response of the sample during gas entry and breakthrough. With this in mind, emphasis was placed on examining the processes and mechanisms governing initial gas penetration of the clay, in particular (i) the minimum pressure that gas became mobile and entered the clay, (ii) the processes governing gas entry and breakthrough (signified by advective gas flow to one of the radial filters) and (iii) the nature of the observed couple between gas flow, gas pressure, local stress and porewater pressure, and its impact, if any, on gas permeability. It should be noted that the duration of each test stage is an artefact of the low permeability of the system, the subtlety of the processes under investigation e.g. capillary versus dilatant flow, and the time-dependent behaviour of these materials. It is also important to note that testing is performed with a view to minimising perturbation of the system/sample, in order to elicit the true underlying material responses by better reflecting representative conditions affecting a deep geological disposal facility. An omission to this approach is the lack of a thermal gradient within the system. However, given the complexities involved in understanding the fundamental controls governing gas migration (Rodwell, 2000) this additional level of complexity was felt unwarranted for the current study and would make deconvolving/decoupling individual processes under such conditions significantly harder.

## 4. Results

### 4.1. Hydration

At the outset, test Mx80-A was configured with helium gas within the central injection filter (Fig. 1) to reduce the possibility of hydraulic ‘slug’ flow from displacement of residual water potentially trapped within the injection system during initial hydration of the clay. However, to promote resaturation and swelling of the sample as a whole, distilled water was introduced into all radial and enclosure filters to maximise the surface area in contact with water. Pressures in the water- and gas-saturated filters were maintained at the same value during this stage. At the onset of testing, pressure in the injection and backpressure systems were initially set at 0.25 MPa, Table 2, to locally hydrate the clay-steel interfaces within the system. This was then increased at day 8.3 to 1.0 MPa (in all filters except EC2) to reduce swelling time and promote quicker hydration of the clay. This pressure was then maintained in all radial filters for the rest of the test. Fig. 2A shows the development of stress and uptake of water during this stage. Inspection of the data shows the time-dependent development of swelling pressure (signified by an increase in stress) which appears to asymptote around 23 days. A mass balance of the system demonstrates that around 1.45 ml of water was injected into the sample. Geotechnical measurements based on the post-test mass of the sample indicate a water

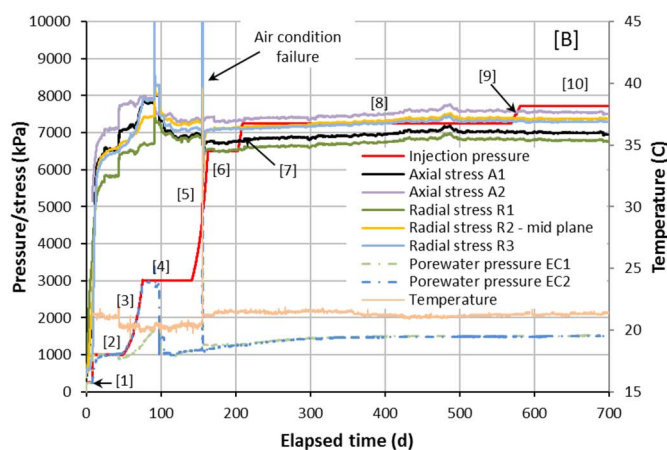
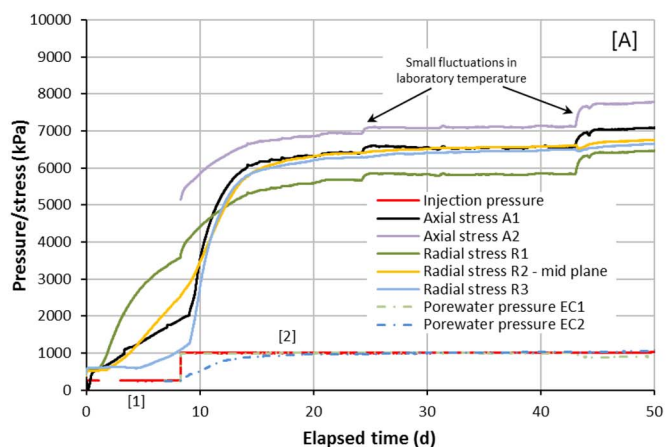


Fig. 2. [A] initial hydration of the bentonite during stages [1] and [2] showing the development of local stress and porewater pressure in response to the swelling of the sample. The increases in stress at day 25 and 43 coincide with a small ( $< 1^\circ\text{C}$  changes in room temperature). [B] Illustrates the initial gas pressurisation history, test stages [3] through [9], showing the local stress and porewater pressure response as a function of time. Spikes in data at days 91 and 155 stem from accidental pressurisation of the filter due to a faulty valve and failure of the air conditioning system respectively. However, inspection of the data indicates any perturbation to the clay caused by these events has no significant effect on the clay or its mechanical properties beyond stage [6].

saturation in excess of 99%. Given this measurement was made after prolonged gas testing, this indicates the sample must have been fully saturated at the end of stage [2].

Common to many laboratory experiments performed on bentonite, examination of the data (Fig. 2A), indicates a heterogeneous stress distribution i.e. stress is non-uniformly distributed within the clay (Harrington and Horseman, 2003; Graham et al., 2012). While the origins of this behaviour remain unclear, relating this often observed heterogeneity in stress to micro-structural models of bentonite behaviour remains a challenge. Further work is required to better understand the relationship between friction (e.g. between the sample and vessel wall), hydraulic equilibrium and possible structural controls on the development of stress. However, at the end of test stage [2] an average stress of 6.8 MPa was measured, resulting in a swelling pressure of 5.8 MPa.<sup>3</sup> The cause for the small increase in stress observed at around day 43 remains unclear. While this coincides with a minor increase in laboratory temperature ( $< 1^\circ\text{C}$ ), a drop in temperature at day 25 also resulted in a small increase in stress. This is difficult to explain from a hydro mechanical (HM) perspective, but strongly suggests that the slow evolution of stress to step changes in temperature are a true

<sup>3</sup> This is in good agreement with data presented by Börgesson et al. (1996) which suggests values in the range 5–6 MPa for the equivalent void ratio used in this study.

material response (possibly related to friction between the sample and vessel wall) rather than the sensitivity of the instrumentation to small-scale thermal fluctuations.

#### 4.2. Gas injection

To investigate the point at which gas becomes mobile in the clay, pressure in the injection system was slowly increased in a step-wise manner, stages [3] through [11], while flux in and out of the system was monitored with time. During each stage, stress and porewater pressure were continuously recorded in order to examine the strength, if any, of the HM coupling between the gas phase and stress.

Gas pressure was initially increased from 1.0 MPa to 7.73 MPa in a series of steps over a 700 day period. During the initial pressure ramp, stage [3], and the first section of stage [4], a faulty valve led to the accidental pressurisation of water in the injection end closure filter (Fig. 1), resulting in a small increase in stress and an outflow of water to the radial filters evidenced by an increase in water pressure in filters EC1 and EC2 (Fig. 2B). This was identified and resolved by day 98 and the pressure in filter EC2 returned to 1 MPa. The filter was then isolated, providing a measure of the porewater pressure within the clay. However, the excess porewater pressure in the sample, caused by this initial event, resulted in continued drainage, leading a small increase in stress (Fig. 2B). This necessitated the depressurisation of this filter (to the reference condition of 1.0 MPa) at day 105. Thereafter, stress within the system began to equilibrate and by the end of stage [4] it had reached an asymptote with an average value of 7.1 MPa, very close to the original value from stage [2]. While this and two other air conditioning failures at days 91 and 155 resulted in some unwanted experimental noise, the data in Fig. 2B indicates that any perturbation to the clay caused by these events had no significant effect on the clay or its mechanical properties beyond stage [6], as illustrated by the consistent stress data.

During test stage [8], stress gradually increased, reaching a well-defined asymptote around day 430. Thereafter stress remained fairly static and did not show any obvious change in value when gas pressure was slowly increased from 7.0 to 7.73 MPa from day 569, stages [9] and [10]. However, the small increase noted in stress is mirrored in a change in porewater pressure in both axial EC1 and EC2 filters, suggesting the change in stress may be driven by the displacement of water from these filters as gas diffuses and then accumulates in the filter porosity. Either way, by the end of stage [10] the system was in some form of quasi equilibrium, with no obvious changes in stress or porewater pressure gradient occurring over the experimental timescale.

Following another thermal outage in the laboratory, an associated gas flow event was observed. However, thorough assessment of the data showed this was not detrimental to the behaviour of the clay as rapid sealing was observed. Gas pressure, porewater pressures and stress within the sample were then allowed to equilibrate (day 700 to 720) before gas pressure was reset to 5 MPa at the start of stage [11]. Pressure in the injection system was then slowly increased by compressing the gas (whose initial volume was around 211 ml) at a constant flow rate of 125  $\mu\text{l/h}$ , Fig. 3. At day 739.2, gas pressure exceeded the minimum stress in the clay (i.e. axial stress A1). However, it is not until day 743.5, when gas pressure exceeds the maximum stress in the system (radial stress R2), that a couple between gas pressure and stress becomes evident, signified by the change in slope of the stress response.<sup>4</sup> This control on gas entry is consistent with observations in fully saturated bentonites (Sellin and Leupin, 2013). As gas pressure continues to slowly increase, all stress sensors exhibit a positive gradient, slowly increasing with gas pressure. The first clear evidence for gas entry occurs at day 747.3, resulting in a series of pathway propagation events.

<sup>4</sup> Given gas is present in axial filters EC1 and EC2 it is not possible to accurately determine porewater pressure, and therefore, the effective stress.

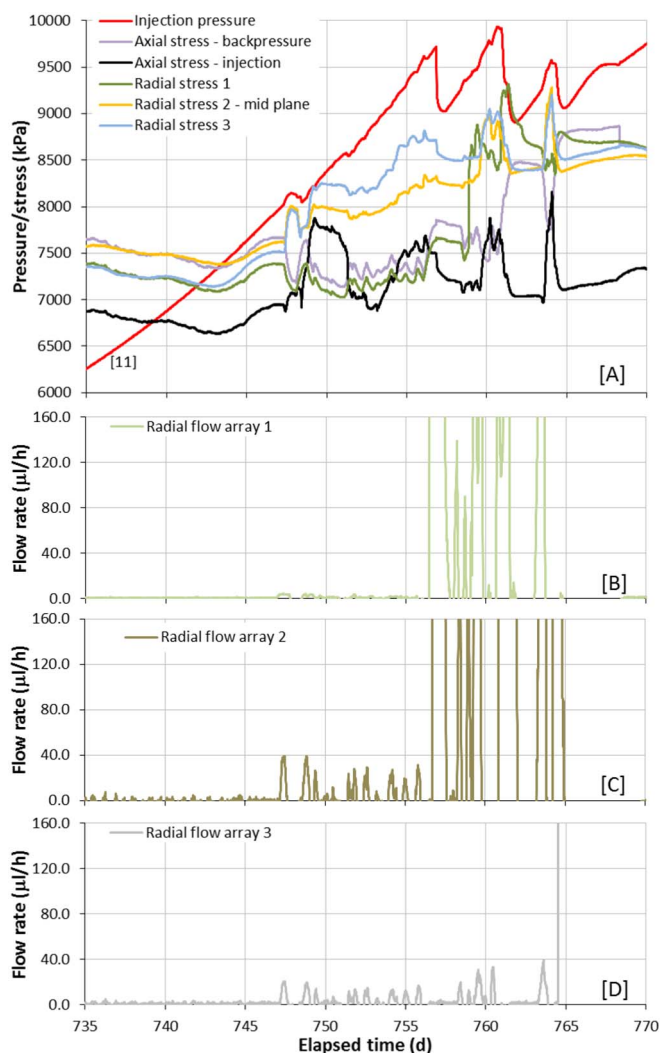


**Fig. 3.** Evolution in gas pressure, stress and outflow during multiple gas breakthrough events. Graph [A] depicts gas pressure and local stress. [B], [C] and [D] show the outflow of gas to radial arrays 1, 2 and 3 respectively. Inflections in stress are indicative of pathway propagation events and are often accompanied by outflow to one or more arrays (Fig. 1). Major gas breakthrough events are noted around days 757, 761 and 764 signified by sudden drops in gas pressure, changes in the distribution of stress and the rapid discharge of gas. Outflow data is time-averaged to help identify underlying trends. This introduces a small time-shift in the data of  $\pm 3$  h which explains why outflow appears to occur marginally before peak gas pressures.

These perturb the stress field within the clay, signified by variance in absolute stress values, which increase or decrease as a function of time (see Discussion). This somewhat chaotic behaviour is thought to relate to specific pathway propagation events as gas penetrates and migrates through the clay, with the magnitude and direction of the stress change strongly linked to the orientation and aperture of the pathway (see event analysis). In this way, each inflection in the gas pressure and stress traces would seem to relate to changes in the geometric configuration of gas pathways as a function of time. This yields a gas entry pressure around 8.05 MPa, which is in line with previous values reported by Graham et al. (2012). Inspection of the data in Fig. 3 [A through D] indicates abrupt changes in stress are often associated with specific discharge events to one or more of the three radial filter arrays, Fig. 1, a detailed analysis of which is contained within the Discussion section. These outflows are both sporadic and non-uniformly distributed through the clay, indicating localised flow through initially unstable pathways, which open and close depending on the local value of gas pressure and stress in the system. This capacity for closure and rapid reduction in outflow highlights the ability of the clay to self-seal

under these circumstances.

This instability in pathway geometry leads to an under-development of gas permeability, constricting flow, which then results in continued gas pressurisation. While a number of minor breakthrough events occur, it is not until day 756.9, at an initial peak gas pressure of 9.48 MPa, that major gas breakthrough finally occurs. This is accompanied by rapid degassing of the clay through arrays 1 and 2 (Fig. 1), resulting in a negative pressure transient to a new gas pressure of 9.29 MPa.

Thereafter gas pressure continues to decline at a slower rate as outflow continues, reaching a minimum value of 9.02 MPa at day 757.4. The inability of these previously conductive pathways to remain open (see Discussion) results in a lack of permanent permeability change within the clay, leading to two further discrete gas breakthrough events at days 761 and 764. Inspection of the data (Fig. 3), shows multiple inflections in stress and outbursts of gas during the second pressurisation event from day 757 to 761, providing further evidence for the instability of these features. The geometric evolution of the permeability field is reflected in the changing distribution of stress state during these events, with both evolving during this phase of testing.

Following the third major gas breakthrough event at day 764, outflows to arrays 1 and 2 cease with flow now focussed to array 3. This phase of the test is accompanied by an apparent reduction in pathway propagation events signified by minimal perturbation of the stress field, exhibited by a much smoother trace. In addition, stresses are seen to generally converge, with the exception of that measured nearest the injection end-closure, which continues to maintain a significant offset to the rest of the stress data. This is probably a legacy from previous flow events, resulting from residual gas trapped within the clay. As gas pressurisation continues from day 765 onwards, Fig. 4, outflow to array 3 varies, spiking again at day 767.8, which is accompanied by an inflection in the gas injection pressure. However, as before, the pathway is unable to remain open, permeability drops and gas pressurisation continues (albeit at a slower rate than before the event). Gas pressure peaks at 9.88 MPa around day 771.7, with flow continuing to be focussed to array 3, Fig. 4. This is followed by a protracted negative pressure transient leading to a quasi-steady state by around day 825. During this period, the change in injection pressure is crudely mirrored in all of the stress sensors, which exhibit none of the chaotic patterns observed with earlier breakthrough events. Gas pressure is now roughly equal to the maximum value of stress in the system, in this case axial stress A2 measured in right closure platen (Fig. 1). While outflow remains focussed to one specific array, the flux remains relatively stable, exhibiting much less variability than before. Outflow to arrays [1] and [2] remain minimal, indicating highly localised gas flow within the bentonite sample.

## 5. Discussion

For gas penetration of precompacted bentonite to occur, two primary mechanisms for advection are available: (i) gas may enter the voidage within the clay, by first displacing porewater or (ii) gas may generate new voidage within the bentonite through the generation of microfractures, resulting in localised consolidation and disruption of the stress field. The experimental data presented in this paper is consistent with (ii), based on evidence for coupling between outflow and stress, as well as the development of a heterogenic stress field during initial gas entry and migration (Fig. 3).

For gas to migrate via this mechanism, it must first create one or more conductive pathways, moving from a system with ostensibly zero advective gas permeability to one in which finite gas permeability exists. In creating this/these pathway/s, and thereby new voidage, the gas must not just break the bonds between the water and the clay but it must also compress the surrounding clay matrix in order to provide the necessary volume required for pathway dilation to occur. While our

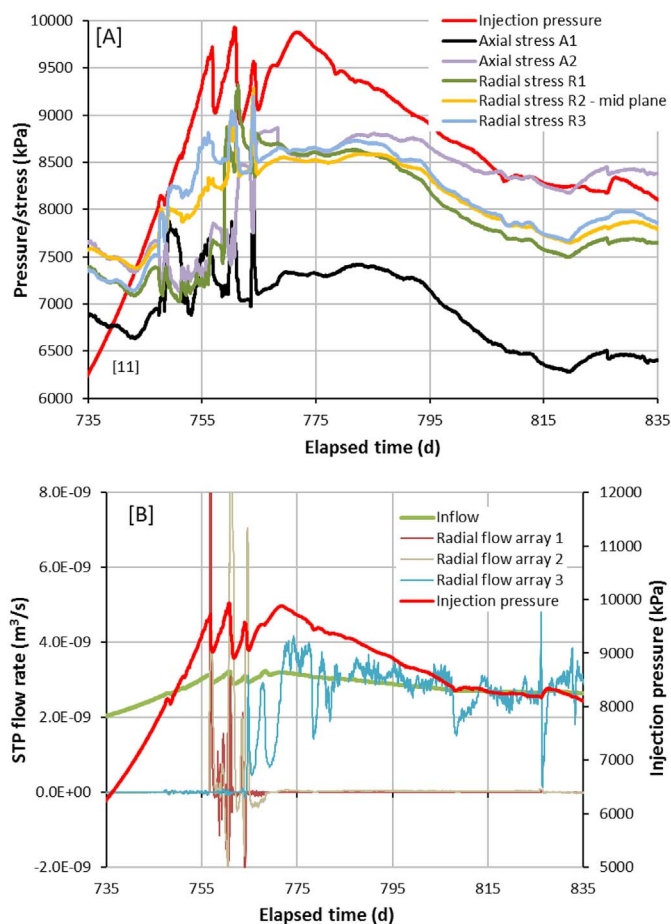


Fig. 4. Injection pressure, stress and out flow data from day 735 to 835, test stage [11]. [A] Illustrates the evolution in stress behaviour from initial gas entry to steady state conditions. The peak in gas pressure (around day 767.6) is followed by a protracted negative pressure transient leading to a quasi-steady state by around day 825. During this period, the change in injection pressure is crudely mirrored by stress which exhibits none of the chaotic patterns observed with earlier breakthrough events. The reduction in the variability of stress from day 768 onwards is accompanied by the development of ‘stable’ outflow conditions [B], with flux localised to one drainage array. Standard temperature and pressure (STP) are defined as 273.15 K, 101.325 kPa respectively.

choice of constant volume boundary condition may influence both peak gas pressure and characteristics of the resulting network, a similar condition will exist in repositories located within hard host rocks which constrain the clay.

### 5.1. Stress analysis

In order to gain further insight into the development of gas pathways within the sample, it is first necessary to uncouple changes in stress resulting from increasing gas pressure (signified by a gradual change in slope, Fig. 3) and transient activity resulting from pathway propagation ‘events’ (apparent as local stress and flow perturbations) by considering the rate at which such changes occur. To do so, the derivative of all stress and flow measurements was found, with respect to time, from day 740 onwards. Flow fluctuations were notably more rapid than observed changes in measured stresses.

Therefore, for ease of comparison between the two data-types, all stress derivatives were first normalised with respect to the largest magnitude derivative, and the same process applied to the flow derivatives. The resulting traces (Fig. 5A) highlight periods where dynamic effects are apparent, both in stress development and outflow at the radial arrays. A significant period of ‘activity’ in stress measurements is detected from around day 746, consistent with the onset of gas entry,

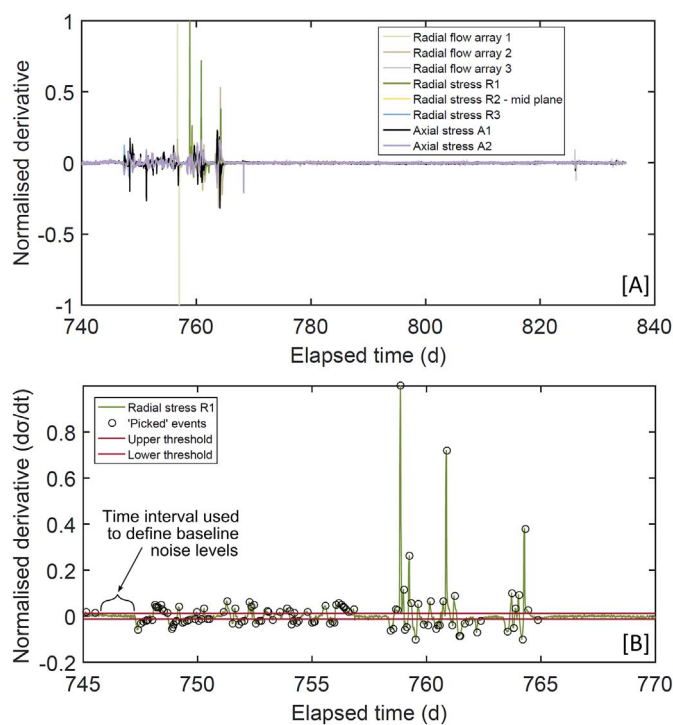


Fig. 5. [A] Normalised derivatives for stress and flow rate time series. Stress fluctuation episodes are apparent for around 10 days before the first major event becomes apparent for flow rate derivatives. A long period of relative ‘quiescence’ was apparent after day 770, where relatively few perturbations were detected in stress and flow rate data. [B] An example of the event detection approach, showing the normalised derivative trace for load cell Radial 1 and the resulting selected perturbation ‘events’. A rolling window is used to assess whether a peak is higher than previous and following windows. The same criterion is applied for troughs, which are selected if below the value found in the bounding windows. To exclude background noise, events (black circles) are only picked if they are observed above or below the upper and lower thresholds respectively.

not long after gas pressure was observed to exceed the maximum stress within the clay. However, only minor changes in outflow behaviour are detected until day 756.9, which corresponds with the observation of major breakthrough. This is followed by several phases of enhanced system development, then a significant reduction in activity and a period of apparent quiescence from day 770 to the end of the test (Fig. 5A), suggesting a decline in pathway propagation events.

Given the constant volume boundary condition, the observed stress field perturbations would seem to imply that gas must deform the clay fabric as it enters the material. Assuming that such fluctuations in stress (and consequent changes in flow) result from individual deformation events, then their quantification has the potential to provide additional insight into pathway development. A simple ‘picking’ algorithm was, therefore, used to assess the timing and magnitude of individual events for all sensors. Stress signals for each sensor first had their initial offset removed and were normalised before finding the first derivative (Fig. 5A). An upper and lower threshold were then set, based on the standard deviation (s.d.) of a manually selected section of the data-set (consisting of 550 data-points) chosen to quantify ‘baseline’ noise levels. The data-set is then repeatedly subsampled in time, using a rolling window (3–4 days long, with an overlap of ¼ of its length). For each window the maximum and minimum values are found and then compared to the previous and following windows in order to select individual signal peaks and troughs. If the selected values occur above or below the chosen noise thresholds they are considered as significant changes in stress gradient and logged as a detected perturbation ‘event’ (Fig. 5B).

Assessment by eye of the resulting ‘picks’ led to the selection of threshold values of  $5 \times \text{s.d.}$  and  $3 \times \text{s.d.}$  for the flow and stress derivatives respectively, at which levels the removal of signal noise was

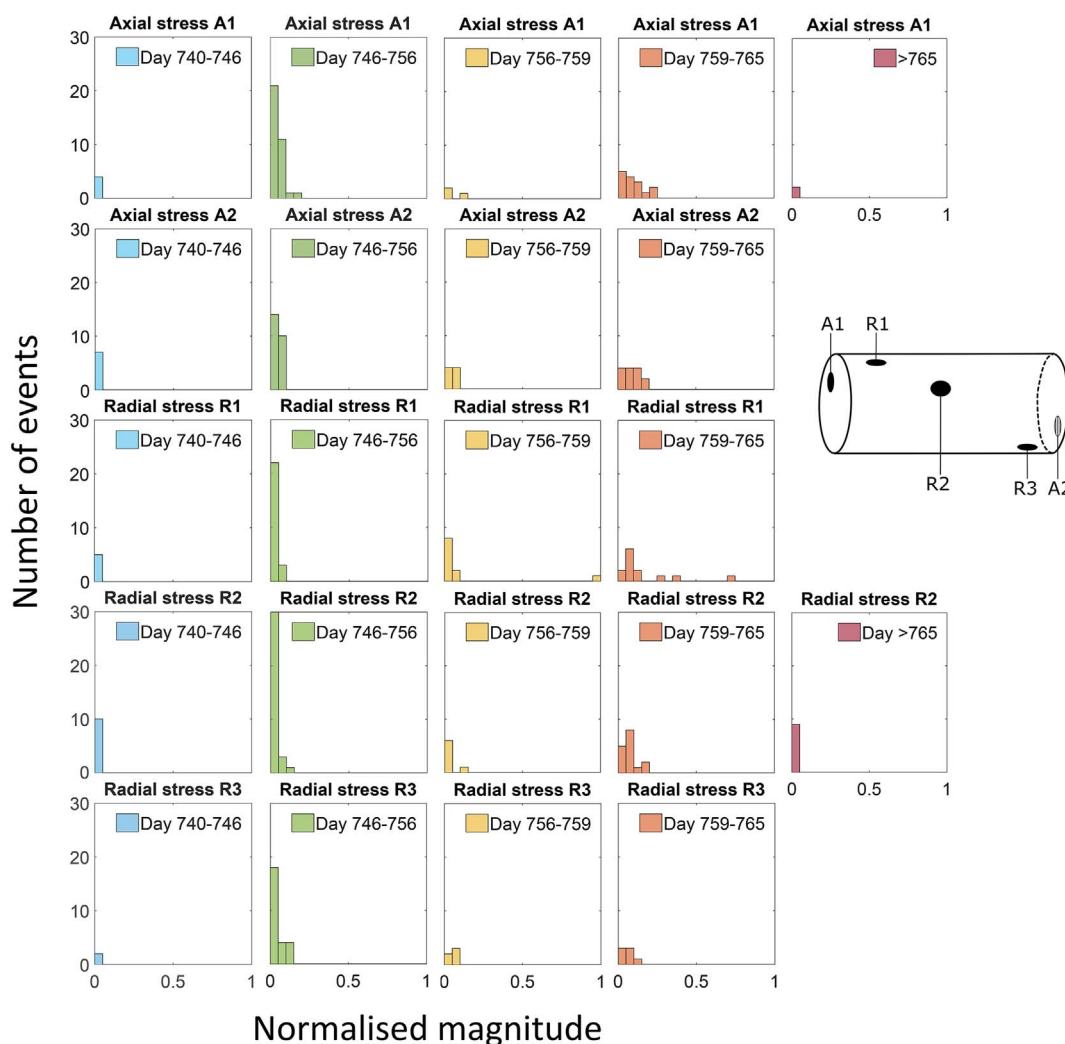


Fig. 6. Magnitudes of stress perturbation events detected at each sensor for selected time periods during testing. Axes x and y denote normalised magnitude and number of events respectively. Each row (1–5) relates to a specific stress sensor, starting from the top with sensors A1, A2, R1, R2 to R3. Each column represents a specific time window starting on the left with days: 740–746 (blue), days 746–756 (green), 756–759 (yellow), 759–765 (orange) and > 765 (red). There were no events detected at sensors A2, R1 and R3 after days 765, so no graphs are given. A schematic shows the position of the stress sensors (right). Two periods of particular activity are seen between days 746–756 and 759–765. An increase in the magnitude of events is also apparent during days 746–756 and particularly between days 759 and 765. (For interpretation of the references to colour in this figure legend, the reader is referred to the web version of this article.)

deemed to be satisfactory. While such an approach may not select every individual event, the results appear highly successful (Fig. 5B) in this case, in that the peaks/troughs of all notable deviations from background noise appear to have been picked correctly, suggesting that the approach might reasonably be considered to have detected the majority of events occurring. Similar automatic algorithms are routinely used in seismology (Leonard and Kennett, 1999) and have proven highly successful in the assessment of micromechanical deformation in the laboratory using acoustic emission data (Zang et al., 1998; Graham et al., 2010). In this case, applying this approach results in the generation of a catalogue of stress disturbance ‘events’, which can then further inform test interpretation. As well as detecting the time of such events, the magnitude of  $do/dt$  is also collected for each of these times, providing an ‘event magnitude’ which relates to the degree of stress field change at the time of occurrence.

To better understand the distribution and degree of stress perturbations occurring during the experiment, histograms were generated showing the magnitude of events detected at each stress sensor, for a range of selected timeframes (Fig. 6). Event histograms for different stages of the experiment are coded by colour. It is immediately apparent that during the early stages of stress perturbation (days 740–746, blue) only a relatively small number of lower magnitude

events are detected at all sensors, particularly radial 3 which is only affected minimally. A more pronounced period of activity (days 746–756, green) then occurs, during which significantly more events are detected, some being of higher magnitude than previously recorded. This is followed by a period of noticeably fewer perturbations (days 756–759, yellow). This is consistent with the observation of a gas pressure minimum occurring at day 757.4 (see Gas injection section), following a period of stress perturbation in advance of major gas breakthrough (at day 756.9). Between days 761 and 764, two further discrete gas flow events occurred, which are associated with an increase in the number of stress fluctuations detected during this time (days 761 and 764, orange). These events display a much larger range of magnitudes. Given that in fracture mechanics, fracture surface area and energy released are directly related (Atkinson, 1987), this indicates the presence of a more established network of pathways, ranging in size. Finally, after day 765, sensors R2 and A1 recorded only a few smaller magnitude events, much as observed during the early stages of stress perturbation (days 740–746), while sensors A2, R1 and R3 detected no disturbances.

This variation in the stress field with time is further demonstrated by plotting event magnitudes for flow (Fig. 7A) and stress (Fig. 7B) against time. A protracted phase of stress disturbance is evidenced

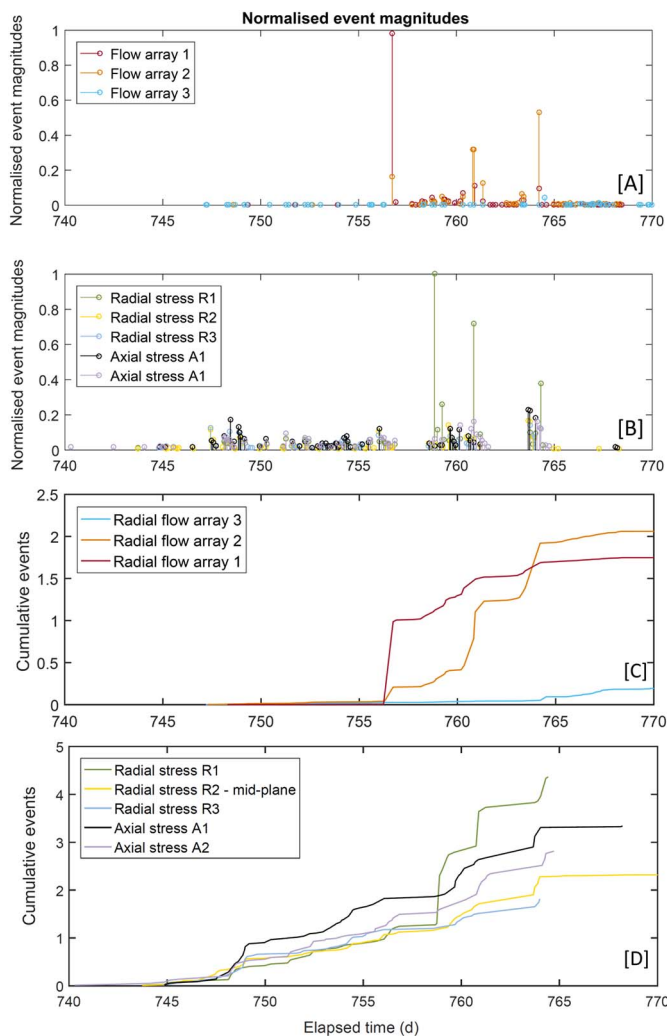


**Fig. 7.** Temporal evolution of stress and flow fluctuations. The magnitude of flow rate [A] and stress events [B] are shown during the most active phase, with respect to time. Several clusters of stress events are apparent during this timeframe. All major flow events follow an intense phase of stress development. In [C & D], the magnitude of all previous events is summed with time, providing a representation of the cumulative activity detected at each sensor/array: [C] relates to flow date and [D] to perturbation in the stress field.

for > 10 days before the first notable outflow disturbances are detected. Three major outflow events are apparent, each associated with a significant degree of perturbation in recorded stresses beforehand. Finally, stress and flow activity settles into a period of ongoing low-level disturbances, not long before peak stress is reached (at day 767.8).

The cumulative magnitude of picked peaks was also found for flow and stress data, with respect to time (Fig. 7C & D). The resulting curves illustrate the relative involvement of different regions of the clay during pathway propagation and associated periods of dynamic flow behaviour. Inspection of the cumulative stress curves again highlights that the first detectable stress ‘events’ were apparent just before and at around 745 days into testing, coincident with the increase in gas pressure above the maximum stress in the system, though the cumulative flow curve shows that the occurrence of major breakthrough occurred sometime later (day 756.9). At around day 760, flow fluctuations become most significant at radial array 2, indicating that the prior phase of pathway propagation was ongoing towards the central plane of the sample. A further burst of activity then occurred, also displaying clear coupling between all stress sensors and outflow at radial array 2. Finally, small magnitude perturbations intensified slightly at radial array 3 at around day 764. From this stage onwards, there is

very little evidence for stress perturbation events in most regions of the sample, indicating that a more stable flow regime had been established (as evidenced by the persistent outflow observed at radial array 3 (Fig. 4) from this stage onwards).

During the 20 days of pathway development following gas pressure exceeding the internal stresses within the clay, all stress sensors experienced significant perturbations. Many of these were not correlated with major outflow events, but appear to have preceded, and likely contributed to, such events. Conversely, no major flow perturbations were detected which did not correlate with fluctuations in the stress field. By the time monitored stresses were observed to homogenise and quiesce, radial load cell 1 had experienced nearly twice the total perturbation detected at radials 2 and 3 (the latter experiencing the least activity), which is consistent with the most pronounced early outflows being detected at radial array 1.

Throughout the period of major stress development, a persistent, moderate level of activity is detected at both axial load cells, which is dominant even after outflow begins at radial array 1. To generate such a signal would require some degree of ongoing fracturing aligned approximately sub-parallel to the end-closure faces, with an opening direction close-to-parallel to the axial load cell faces. Stress perturbations at the radial stress sensors then suggest a complex series of deformation events, starting at the injection point, before progressing to radial arrays [1], [2] and [3] in succession. These observations are highly indicative of a complex network of several interacting fractures/pathways, spatially evolving as the system continues to be energised.

### 5.2. Implications

Observations presented in this paper demonstrate gas migration in saturated and precompacted bentonite occurs through the creation of new voidage within a dilatant gas flow network. Evidence includes the observation of: (i) disturbance of the measured stress field once gas entry has occurred, under a constant volume boundary condition, (ii) the occurrence of localised gas flow within the clay, and (iii) a clear association between episodes of stress field disturbance in advance of gas outflow events. The data shows that bentonite exhibits strongly time-dependent behaviour which will control the development of permeability through its interaction with the stress field and variations in applied gas pressure. In such a scenario, the bulk permeability of the clay must intuitively be linked to the density and aperture distribution within the gas flow network. However, information in relation to these characteristics is not currently available. Further work will therefore be required before numerical models can better represent these processes. It is also clear from the data that once sufficient time has elapsed for the gas phase to ‘rework’ the clay, the heterogeneity within the stress field reduces, with all sensors thereafter following a similar path to that described by the injection gas pressure.

Given this need to create new voidage and the relatively low compressibility of the clay, the requirement for ‘reworking’ would likely result in a period of instability signified by the propagation of multiple pathways, opening and closing as a result of small variations in their internal gas pressure.

Evidence from this study is consistent with the hypothesis that in a hard rock hosted repository, should advective gas flow occur through a bentonite EBS, a threshold criteria must first be met where gas pressure exceeds the local stress experienced by the clay. As a consequence gas pressures will interact with the surrounding rock. Assuming these pressures remain within the elastic domain of the host rock, they are unlikely to have a significant mechanical impact. Nevertheless, they should be considered during repository design and the development of infrastructure.

In this study, we observe for the first time the initial gas network development and associated changes in outflow and stress, over an extended period of time. A period of unstable gas pressure (Fig. 4) is observed until sufficient drainage is found. This differs from previous

observations performed under similar boundary conditions (Harrington and Horseman, 2003), though the reason for this remains unclear. If the gas network cannot access sufficient drainage routes, then a period of further network growth is likely to occur. This will result in an increase in gas pressure until further drainage is found. In an engineered barrier, when a network of pathways forms, its characteristics must be strongly related to the availability of drainage sinks (e.g. fractures intersecting a deposition hole), which will control and therefore regulate gas pressure within the repository.

In order to effectively forecast gas behaviour in such a scenario, the distribution and characteristics of this network must be better understood. However, the controls on the long-term evolution and stability of these networks are as yet unclear. Further work is required to quantify the influence of flow rate on the mobility of gas, the importance of the boundary condition on the stability of gas pathways and role of drainage availability in moderating gas pressures.

## 6. Conclusions

A free gas phase is likely to form in many radioactive waste repository concepts. In a GDF for high-level radioactive waste, pre-compacted bentonite is used to isolate the waste-forms and seal galleries/shafts. It is therefore important to understand the advective flow behaviour in these materials, its impact, and its importance for safety case development. Findings are presented from a high quality, highly instrumented experimental study in precompacted bentonite, designed to examine the coupling between gas flow and the stress field in such a situation.

For the first time we present a detailed analysis of stress field data during the generation and evolution of a gas network. Analysis shows that advective gas flow is strongly coupled to the stress field experienced by the clay. Experimental observations are best explained by the dilatant formation of gas pathways, propagating through the clay in response to variations in applied gas pressure. Findings demonstrate that this behaviour will occur where the EBS is constrained by a stronger host rock.

Quantitative analysis of individual stress perturbation events provides additional insight into the relative involvement of different regions of the clay during pathway propagation. In particular, significant periods of stress field disturbance are apparent in advance of all major gas outflow events and highlight the necessity to propagate an effective gas network before gas escape can occur. Conversely, no major flow perturbations were detected which did not correlate with fluctuations in the stress field. Observations indicate a network of several interacting fractures/pathways, spatially evolving as the system is energised. As gas permeability develops the favoured flow pathway can change, demonstrating the potential for these features to self-seal and highlighting their initial instability, as the network develops. Gas permeability under these conditions must, therefore, be time-dependent in nature.

As steady-state flow is approached, both detected perturbations and heterogeneity within the stress field reduce, indicating that sufficient time has elapsed for the gas phase to develop an established flow network. The density, orientation and aperture of these pathways must directly influence the bulk permeability of the bentonite. However, the controls on the geometry and distribution of such a network is still unclear, as well as its long-term evolution and stability. This understanding would be beneficial for the assessment of gas pressure evolution and its impact on repository infrastructure.

## Acknowledgements

The project was sponsored by the Radioactive Waste Management Ltd. and the British Geological Survey (aligned to the BGS Geosphere Containment Project). Experiments were conducted in the Transport Properties Research Laboratory (TPRL), part of the Fluid Processes

Research Group. The authors would also like to thank Mr. Humphrey Wallis and colleagues from the BGS Research & Design workshops who contributed to the design and manufactured the bespoke equipment used in this study, Mrs. Fiona McEvoy and the anonymous reviewers for their time and constructive comments. The views expressed herein do not necessarily represent those of the funding organisation. This paper is published with permission from the Executive Director of the British Geological Survey.

## References

- Amann-Hildenbrand, A., Krooss, B.M., Harrington, J.F., Cuss, R.J., Davy, C., Skoczylas, F., Jacobs, E., Maes, N., 2015. Chapter 7 - gas transfer through clay barriers. In: Tourmassat, C., Steefel, C.L., Bourg, I.C., Bergaya, F. (Eds.), *Natural and Engineered Clay Barriers. Developments in Clay Science*, vol. 6. pp. 227–267. <http://dx.doi.org/10.1016/B978-0-08-100027-4.00007-3>.
- Angeli, M., Soldal, M., Skurtveit, E., Aker, E., 2009. Experimental percolation of supercritical CO<sub>2</sub> through a caprock. *Energy Procedia* 1, 3351–3358.
- Atkinson, B.K., 1987. *Fracture Mechanics of Rock*. Elsevier.
- Börgesson, L., Karnland, O., Johannesson, L.-E., 1996. Modelling of the physical behaviour of clay barriers close to water saturation. *Eng. Geol.* 41, 127–144.
- Clayton, C.J., Hay, S.J., 1992. Gas migration mechanisms from accumulation to surface. *Bull. Geol. Soc. Denmark* 41, 1223.
- Cuss, R.J., Harrington, J.F., Noy, D.J., Graham, C.C., Sellin, P., 2014a. Evidence of localised gas propagation pathways in a field-scale bentonite engineered barrier system; results from three gas injection tests in the large scale gas injection test (Lasgit). *Appl. Clay Sci.* 102, 81–92. <http://dx.doi.org/10.1016/j.clay.2014.10.014>.
- Cuss, R.J., Harrington, J., Giot, R., Auvray, C., 2014b. Experimental observations of mechanical dilation at the onset of gas flow in Callovo-Oxfordian claystone. In: Norris, A., Bruni, J., Cathelineau, M., Delage, P., Fairhurst, C., Gaucher, E.C., Hohn, E.H., Kalinichev, A., Lallieux, P., Sellin, P. (Eds.), *Clays in Natural and Engineered Barriers for Radioactive Waste Confinement*. vol. 400. Geological Society Special Publications, London, United Kingdom, pp. 507–519. <http://dx.doi.org/10.1144/SP400.26>. Geological Society of London.
- Donohew, A.T., Horseman, S.T., Harrington, J.F., 2000. Chapter 18 gas entry into unconfined clay paste between the liquid and plastic limits. In: *Environmental Mineralogy. Mineralogical Society Series No. 9*. pp. 369–394 (London).
- Gensterblum, Y., Ghanizadeh, A., Cuss, R.J., Amann-Hildenbrand, A., Krooss, B.M., Clarkson, C.R., Harrington, J.F., Zoback, M.D., 2015. Gas storage capacity and transport in shale gas reservoirs – a review; Part A: transport processes. *Journal. Unconv. Oil Gas Resour.* 12, 87–122. <http://dx.doi.org/10.1016/j.juogr.2015.08.001>.
- Gerard, P., Harrington, J., Charlier, R., Collin, F., 2014. Modelling of localised gas preferential pathways in claystone. *Int. J. Rock Mech. Min. Sci.* 67, 104–114.
- Graham, C.C., Stanchits, S., Main, I.G., Dresen, G., 2010. Comparison of polarity and moment tensor inversion methods for source analysis of acoustic emission data. *Int. J. Rock Mech. Min. Sci.* 47 (1), 161–169.
- Graham, C.C., Harrington, J.F., Cuss, R.J., Sellin, P., 2012. Gas migration experiments in bentonite: implications for numerical modelling. *Mineral. Mag.* 76 (8), 3279–3292.
- Harrington, J.F., Horseman, S.T., 1999. Gas transport properties of clays and mudrocks. In: Apelin, A.C., Fleet, A.J., Macquaker, J.H.S. (Eds.), *Muds and Mudstones: Physical and Fluid Flow Properties*. vol. 158. Geol. Soc. London, Spec. Pub., pp. 107–124.
- Harrington, J.F., Horseman, S.T., 2003. Gas migration in KBS-3 buffer bentonite: sensitivity of test parameters to experimental boundary conditions. In: Report TR-03-02. Svensk Kärnbränslehantering AB (SKB), Stockholm, Sweden.
- Harrington, J.F., Noy, D.J., Horseman, S.T., Birchall, J.D., Chadwick, R.A., 2009. Laboratory study of gas and water flow in the Nordland Shale, Sleipner, North Sea. In: Grobe, M., Pashin, J.C., Dodge, R.L. (Eds.), *Carbon Dioxide Sequestration in Geological Media—State of the Science: AAPG Studies in Geology*. 59. pp. 521–543.
- Harrington, J.F., Milodowski, A.E., Graham, C.C., Rushton, J.C., Cuss, R.J., 2012a. Evidence for gas-induced pathways in clay using a nanoparticle injection technique. *Mineral. Mag.* 76 (8), 3327–3336. <http://dx.doi.org/10.1180/minmag.2012.076.8.45>. December 2012.
- Harrington, J.F., de La Vaissière, R., Noy, D.J., Cuss, R.J., Talandier, J., 2012b. Gas flow in Callovo-Oxfordian clay (COx): results from laboratory and field-scale measurements. *Mineral. Mag.* 76 (8), 3303–3318.
- Horseman, S.T., Harrington, J.F., 1994. Migration of repository gases in an over-consolidated clay. British Geological Survey, British Geological Survey. In: Technical Report WE/94/7.
- Horseman, S.T., Harrington, J.F., Sellin, P., 1999. Gas migration in clay barriers. In: Pusch, R., Yong, R.N. (Eds.), *Microstructural Modelling of Natural and Artificially Prepared Clay Soils with Special Emphasis on the use of Clays for Waste Isolation (1999 Special Edition)*, Engineering Geology. Vol. 54. Elsevier, Amsterdam, pp. 139–149.
- Johannesson, L.-E., 2014. Manufacturing of buffer and filling components for the Multi Purpose Test. Svensk Kärnbränslehantering AB (SKB), report P-14-7, (ISSN 1651-4416).
- Judd, A.G., Sim, R.H., 1998. Shallow gas migration mechanisms in deep water sediments. In: Proc. S.U.T. Conference on Offshore Site Investigation and Foundation Behaviour, pp. 163–173.
- Leonard, M., Kennett, B.L.N., 1999. Multi-component autoregressive techniques for the analysis of seismograms. *Phys. Earth Planet. Inter.* 113 (1–4), 247–263 1999.

- Mandl, G., Harkness, R.M., 1987. Hydrocarbon migration by hydraulic fracturing. In: *Deformation of Sediments and Sedimentary Rocks*. vol. 29. Geol. Soc. Special Pub., pp. 39–53.
- Marschall, P., Horseman, S., Gimmi, T., 2005. Characterisation of gas transport properties of the opalinus clay, a potential host rock formation for radioactive waste disposal. *Oil & Gas Science and Technology - IFP International Workshop*. Rev. IFP, vol. 60. pp. 121–139 (2005), No. 1.
- Norris, S., 2015. EC FORGE project: updated consideration of gas generation and migration in the safety case. vol. 415(1). Geological Society, London, pp. 241–258 (Special Publications).
- Ortiz, L., Volckart, G., Mallants, D., 2002. Gas generation and migration in Boom Clay, a potential host rock formation for nuclear waste storage. *Eng. Geol.* 64, 287–296.
- Research into gas generation and migration in radioactive waste repository systems (PROGRESS project). In: Rodwell, W.R. (Ed.), *Nuclear Science and Technology EUR 19133 EN*. European Commission, Luxembourg.
- Romero, E., Senger, R., Marschall, P., 2012. Air injection laboratory experiments on Opalinus clay. In: *Experimental techniques*. 3rd EAGE Shale Workshop, Barcelona, Spain, 23–25 January 2012, Results and Analyses.
- Sellin, P., Leupin, O.X., 2013. The use of clay as an engineered barrier in radioactive-waste management – a review. *Clay Clay Miner.* 61 (6), 477–498.
- Skurtveit, E., Aker, E., Soldal, M., Angeli, M., Wang, Z., 2012. Experimental investigation of CO<sub>2</sub> breakthrough and flow mechanisms in shale. *Pet. Geosci.* 18, 3–15. <http://dx.doi.org/10.1144/1354-079311-016>.
- Svensk Kärnbränslehantering AB (SKB), 2006. Buffer and Backfill Process Report for the Safety Assessment SR-Can. Technical Report TR-06-18. <http://www.skb.se/publication/1174786/TR-06-18.pdf>.
- Tissot, B., Pellet, R., 1971. Nouvelles données sur les mécanismes de genèse et de migration du pétrole: simulation mathématique et application à la prospection. In: *Proceedings of the 8th World Petroleum Congress, Moscow*, pp. 35–46.
- Weetjens, E., Sillen, X., 2006. Gas generation and migration in the near field of a supercontainer-based disposal system for vitrified high-level radioactive waste. In: *Proc. 11th Int. High-Level Radioactive Waste Management Conf. (IHLRWM)*, Las Vegas, Nevada, April 30–May 4, 2006.
- Whitlow, R., 2001. *Basic Soil Mechanics*. Prentice Hall.
- Wikramaratna, R.S., Goodfield, M., Rodwell, W.R., Nash, P.J., Agg, P.J., 1993. A preliminary assessment of gas migration from the copper/steel canister. In: SKB Technical Report TR93–31.
- Wiseall, A.C., Cuss, R.J., Graham, C.C., Harrington, J.F., 2015. The visualization of flow paths in experimental studies of clay-rich materials. *Mineral. Mag.* 79 (6), 1335–1342.
- Zang, A., Wagner, C., Stanchits, S., Dresen, G., Andresen, R., Haidekker, M.A., 1998. Source analysis of acoustic emissions in Aue granite cores under symmetric and asymmetric compressive loads. *Geophys. J. Int.* 135, 1113–1130.